



Research Paper

Experimental characterization of the heat transfer coefficient under different close loop controlled pressures and die temperatures

Joseba Mendiguren ^{*}, Rafael Ortubay, Eneko Saenz de Argandoña, Lander Galdos

Department of Mechanical and Industrial Production, Mondragon Unibertsitatea, Loramendi 4, Mondragon, Gipuzkoa 20500, Spain



HIGHLIGHTS

- Press hardening heat transfer during quenching has been studied.
- Rigorous experimental data has been obtained on quenching times.
- Variable HTC has been defined for press hardening process FEM optimization.
- The HTC has been characterized with high temperature dies for tailor quenching press hardening.
- Valuable data for process time reduction has been obtained and an analytical model proposed.

ARTICLE INFO

Article history:

Received 25 October 2015

Accepted 24 January 2016

Available online 4 February 2016

Keywords:

Heat transfer coefficient

Press hardening

Hot stamping

Contact pressure

Quenching

Tailor quenching

ABSTRACT

The prediction of the final microstructure on press hardening processes strongly depends on the heat transfer kinetics that cools down the blank and governs its martensitic transformation. The main objective of the work is to rigorously and in a systematic manner analyse the influence of the contact pressure and die temperature on the heat transfer coefficient (HTC) for press hardening applications.

The columnar experimental set-up used in this work is presented and the efficient analytical/numerical methodology developed for the surface temperature, heat flux and therefore HTC identification are shown. From the present analysis it is concluded that the HTC critically varies during the cooling process. In the same way the strong dependency of the results on the contact pressure and their weak dependency on the die temperature are shown. An analytical model to represent the HTC evolution on press hardening simulation is presented.

This work presents a valuable set of experimental data regarding the HTC characterization.

© 2016 Elsevier Ltd. All rights reserved.

1. Introduction

The tightening of the international policies on vehicle weight reduction and safety increase has forced automotive industry to a challenging position in the last years. On the one hand, the amount of material on the car body has to be reduced in order to decrease weight and therefore fuel consumption. In this way, a more sustainable product can be achieved reducing gas emissions and allowing a cost saving. On the other hand, in order to fulfil the international safety requirements (EuroNCAP, US-NCAP, JNCAP, FMVSS) the body-in-white (BIW) has to increase in strength while maintaining, if not increasing, as well its crash energy absorption ability.

In order to achieve these goals, two different strategies have been followed by the industry. On the one hand, the use of high strength steels in the range of 600 MPa to 1200 MPa [1], by increasing the strength of the material the volume, is decreased. However, these

new alloys required important forming forces and they have formability limitations [2]. On the other hand, using the press hardening technology, a high Mn content steel (usually 22MnB5) is formed after pre heating up to 900–950 °C and then quenched on the dies leading to high strength martensitic component (with strengths up to 1500 MPa) with a week springback [3]. In addition this technology allows the optimization of part properties via tailor-quenching press hardening process. In this process, a heterogeneous cooling rate is generated on the quenching step in order to lead to different microstructures along the part and therefore different mechanical properties [4].

One of the main drawbacks of this technology is the complex physical phenomena involved i.e. plastic forming, heat transfer, microstructure changes. Therefore, the process optimization becomes a complicated task and usually requires high complexity finite element method (FEM) simulations to define the adequate process parameters. The commercial 22MnB5 alloy of Arcelor (USIBOR 1500P) was thermo-mechanically characterized by Merklein and Lechler showing that due to the high sensitivity on temperature and strain rate of the material it is critical to take into account these

^{*} Corresponding author. Tel.: +34 944301685; fax: +34 943791536.
E-mail address: jmendiguren@mondragon.edu (J. Mendiguren).

phenomena on press hardening simulations [5]. In the same context, Guler and Ozcan [6] stated the importance of the heat transfer accurate modelling on the U channel press hardening FEM numerical model definition.

The heat transfer kinetics between two bodies in contact is governed by the heat transfer coefficient (HTC), which relates the temperature difference on the interface with the heat flux through that interface [7]. Lenard and Davis [8] studied the HTC for flat hot rolling and compression processes on their early work and they found the HTC to be strongly dependent on the interface pressure and temperature. In order to characterize the HTC from a more scientific point of view, Malinowski et al. [9] developed a new testing methodology in which two stainless steel AISI303 dies were put in contact. One of them was previously heated to temperatures between 300 °C and 900 °C while the other one was at room temperature. Helped with FEM models, they analysed the HTC under different pressures from 30 MPa up to 90 MPa leading to values ranging from 50 to 20,000 W/Km².

Aimed at increasing the temperature measuring accuracy, Chang and Bramley [10], developed a robust surface thermocouple to measure temperature at the workpiece–die interface and they characterized the HTC between AISI H13 dies and billets of BS080M40 at 910 °C for forging operations. They concluded that during the quenching stage the HTC could be considered constant but that during the forming stage the HTC had a strong dependency on the interface condition. Similar conclusion was stated by Salomonsson et al. [11], who combined experimental and numerical work to analyse the HTC in a press hardening process for two different 22MnB5 materials under 1 MPa, 10 MPa and 20 MPa pressures. On the other hand, Tondini et al. [12] studied the HTC between USIBOR 1500P and four different die materials (AISI H11, 99.5% alumina, glass-ceramic Macor and Y-PZ) in a range between 5 MPa and 40 MPa, concluding a weak relation between the HTC and the temperature, at least in the interval of temperatures of interest, and therefore stating that the HTC was only dependent on the contact pressure.

The heat transfer kinetics between the USIBOR 1500P and the Z160CDV12 die material was studied by Abdulhay et al. in two subsequent works. On the first work [13], they presented an experimental procedure based on a U channel drawing tooling in which the heat transfer kinetics was monitored and the HTC was characterized by analytically solving the involved thermal equations. They were able to identify the singularity on the HTC values due to the dissipative energy generated during the martensite transformation leading to a power law evolution of the HTC function of the contact pressure. On the second work [14], they presented a press-hardening numerical model in which not only the convection with the ambient air but also the radiation with the air, punch and die were taken into account during the rest on die stage simulation.

A new simple on-dimensional analytical model to determine the HTC was presented by Bai et al. [15] for Ti-6Al-4V upsetting operations. The new methodology was numerically validated using FEM and they concluded that the HTC increases with the applied pressure. In a subsequent work [16] the influence of the surface roughness was analysed, noticing a reduction of the HTC with the increase of the roughness.

Merklein and Lachler [17] associated the pressure dependency of the HTC to the increase of the effective contacting surface between the contact surfaces due to the smoothing of the surface. The same concept was studied by Caron, Daun and Wells [18] and Wang et al. [19] developing numerical models able to take into account the microplastication of the surface and the air gap conductance of the voids created between the rough surfaces.

Summarizing, the HTC dependence on the contact pressure has been widely proved by previous authors who related this

phenomenon to the microplastication of the contact surfaces. However, discrepancies exist about the variation of the HTC during the cooling process and it is not clear if this phenomenon is temperature dependent, pressure variation during cooling dependent or other uncontrolled experimental parameter dependent.

The objective of the present work is the characterization of the heat transfer coefficient (HTC) under different constant, close loop controlled, pressures and die temperatures for press hardening manufacturing processes. This investigation is the first study that analyses rigorously and in a systematic manner the influence of the contact pressure and the die temperature on the temperature and heat flux evolution during the press hardening cooling process. First, the columnar experimental set-up used in this work is presented and the studied pressure and temperature ranges are defined. Next, the analytical/numerical methodology developed for the surface temperature, heat flux and therefore HTC identification is shown. Then, experimental temperatures, calculated surface temperatures and heat flux during each cooling stage are presented. Finally, HTC evolutions are shown and the main conclusions are drawn.

2. Experimental set up

In order to emulate the press hardening process, a laboratory schematic prototype based on Bai et al.'s experimental set up [16] for forging upsetting operations was constructed using ORVAR SUPREME tool steel material (surface roughness around 0.7 μm). As shown in Fig. 1, the prototype consists of two symmetric 50 mm diameter cylindrical shape dies where a 30 mm diameter workpiece is placed between them. In this work, the workpiece is a 1.8 mm thickness Arcerlor's boron steel USIBOR 1500P (surface roughness around 0.45 μm).

The dies are equipped with heating cartridges and control thermocouples in order to be able to establish a close loop heating control covering temperatures in a range of 24–650 °C. The set-up is mounted in a high precision micro-press Schmidt 420 with a close loop pressure control with a resolution of 0.0032 MPa.

A data acquisition system, National Instruments 9215 hardware at 50 Hz, has been used in order to record the temperature evolution during the whole process. Four TC Direct 12-K-1000-118-1-21-3P2L-1A30, 1 mm diameter thermocouples, have been used to measure the temperature evolution on the lower die. These thermocouples are located to 2 mm, 4 mm, 6 mm and 8 mm from the interface between the workpiece and the lower die as represented on Fig. 1b. On the workpiece on the other hand, and due to the limited space on the thickness, a single 0.5 mm diameter thermocouple (12-K-1000-118-0.5-2I-3P2L-1A30) on the middle of the thickness has been used. The hole for the thermocouple in the workpiece is critical and electric discharge machining (EDM) has been used for its preparation.

The experimental procedure is defined as follows. First, the workpiece is heated in an electrical resistance furnace to 950 °C. In order to allow the complete austenitization of the material, the temperature is maintained then during 5 min (temperature is monitored with the workpiece thermocouple). Next, the transfer of the workpiece from the furnace to the die is performed positioning this one on the lower die as shown in Fig. 1a. Finally, the stamping process is conducted imposing a specific pressure on the material during the quenching.

In order to analyse the influence of the applied pressure and the die temperature, experiments were carried out in a range between 1 MPa and 15 MPa and the tool's temperatures are between 24 °C and 450 °C. These test conditions are summarized on Table 1.

The whole range of pressures was studied under 24 °C and 450 °C die temperatures while 10 MPa was used as a benchmark pressure for the die temperature influence analysis. The heat transfer

Table 1
Experimental trial pressures and temperatures.

Pressure (MPa)	Temperature (°C)
1	24
3	80
4	200
10	300
15	450

analysis with high tooling temperatures (200–450 °C) takes importance for tailor press hardening operations in where the tool is partially heated to create soft zones in the part.

3. Numerical determination of the heat transfer coefficient (HTC)

The heat transfer coefficient (HTC) is mathematically defined as the ratio between the heat flux through the interface and the temperature difference [7],

$$HTC = \frac{Q}{T_{w1} - T_{d1}}, \tag{1}$$

where Q is the heat flux through the interface and T_{w1} and T_{d1} are the temperature at the surface of the workpiece and the temperature at the surface of the die respectively.

Fig. 2 represents the temperature data points of the set-up. The d subindex indicates that the temperature points belong to the die while the w index belongs to the workpiece. T_{w2} represents the temperature point on the middle of the thickness measured by the thermocouple while $T_{d2}, T_{d3}, T_{d4}, T_{d5}$ are the die temperatures measured by the thermocouples at 2 mm, 4 mm, 6 mm and 8 mm from the die surface respectively.

The experimental data T_{w2} and T_{d2-5} are known while T_{w1} and T_{d1} (temperatures on the surfaces) are needed for the HTC calculation. In this regard, it is assumed that the heat conduction on the die is governed by the Fourier's law

$$\frac{\partial T}{\partial t} = \alpha_d \left(\frac{\partial^2 T}{\partial x^2} \right), \tag{2}$$

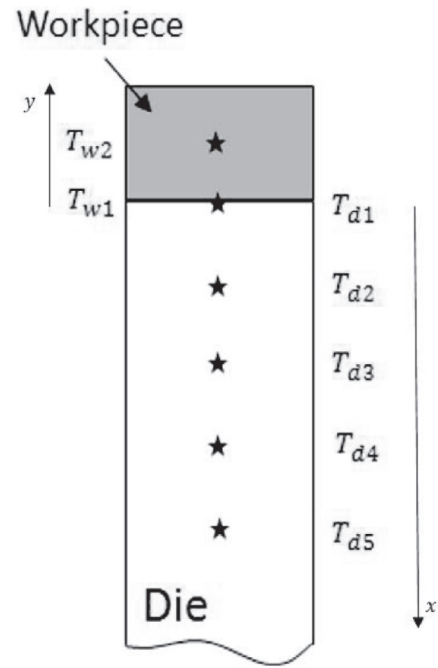


Fig. 2. Schematic representation of the temperature points on the die (T_{di}) and workpiece (T_{wi}) where the first points (T_{d1} and T_{w1}) represent the temperature on the contact surface.

where t represents time, x represents the distance from the interface surface and the material property coefficient α_d is defined as

$$\alpha_d = \left(\frac{k_d}{\rho_d c_d} \right), \tag{3}$$

k_d being the thermal conductivity, ρ_d the density and c_d the specific heat. In order to numerically calculate the temperature at the surface of the die, T_{w1} , the partial derivative of the temperature to the time, $(\frac{\partial T}{\partial t})$, of the conduction equation (Eq. 2) is replaced by the first order backward difference, and the spatial second partial derivative, $(\frac{\partial^2 T}{\partial x^2})$, is replaced by the BTCS method. Therefore the numerical approximation of Eq. (2) results on

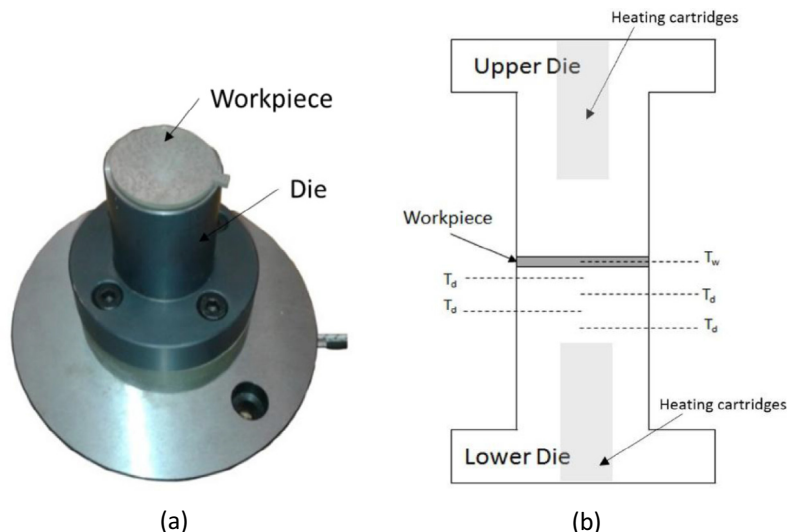


Fig. 1. Columnar experimental set-up: a) Columnar device and b) schematics of the thermocouple identification.

Table 2
USIBOR 1500P boron steel thermal properties [18].

Property	Austenite	Martensite
Specific heat C_p (J/kg °K)	426.0+0.1538 T	311.2+0.439 T
Thermal conductivity k (W/m °K)	16.27+0.010 T	83.73–0.245 T +5.79×10 ⁻⁴ T ² –5.18×10 ⁻⁷ T ³
Density ρ (kg/m ³)	7830	7830

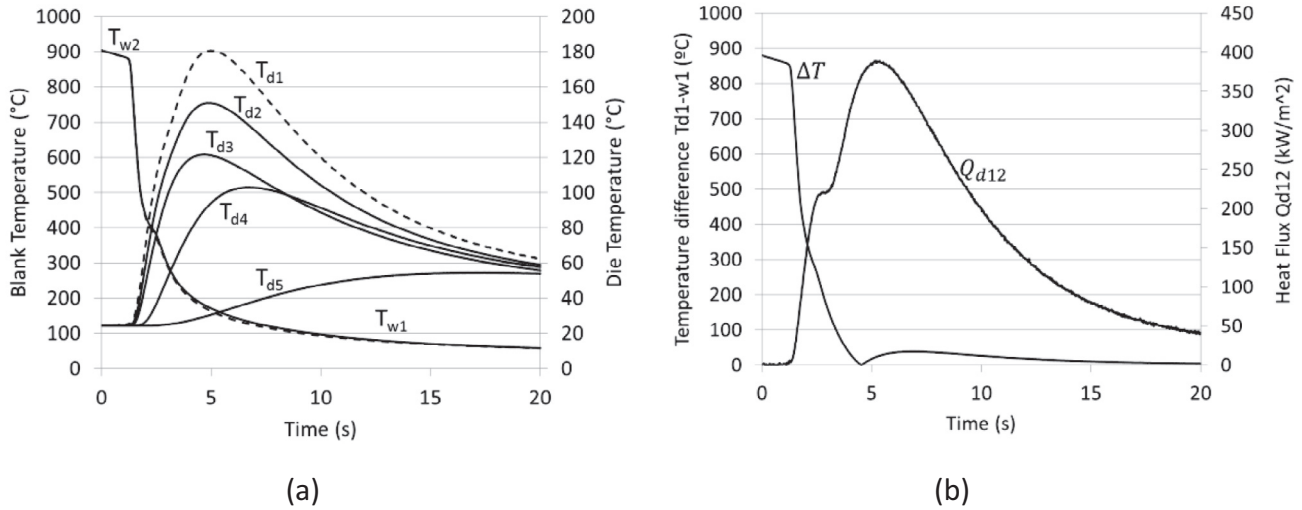


Fig. 3. Heat transfer analysis characteristic result: a) temperature evolution and b) flux and temperature difference representation.

$$\left(\frac{T_{d,i}^{n+1} - T_{d,i}^n}{\Delta t} \right) = \alpha_d \left(\frac{T_{d,i-1}^{n+1} - 2T_{d,i}^{n+1} + T_{d,i+1}^{n+1}}{(\Delta x)^2} \right) + o(\Delta t) + o(\Delta x^2), \quad (4)$$

where $T_{d,i}^{n+1}$ represents the temperature on the (i) -th point at the $(n+1)$ increment. The time step from increment to increment is represented as Δt , while the space increment from point to point is represented as Δx . For the development of the numerical model the discretization shown in Eq. (4) has been truncated neglecting the error terms $o(\Delta t)$ and $o(\Delta x^2)$. These assumptions lead to a first order approximation on time and a second order approximation on space. Supposing Dirichlet boundary conditions (the initial temperature of the surface $T_{d,1}^1$ is the same as the initial temperature of the first thermocouple $T_{d,2}^1$) the problem to solve leads to know the temperature at the surface at the end of the increment, $T_{d,1}^{n+1}$.

From Eq. (4) the following mathematical relations can be obtained for the $T_{d,2}$ temperature point,

$$\frac{\Delta T_{d,2}}{\Delta t} = \frac{\alpha_d}{(\Delta x)^2} (T_{d,1}^{n+1} - 2T_{d,2}^{n+1} + T_{d,3}^{n+1}). \quad (5)$$

For the $T_{d,3}$ temperature point,

$$\frac{\Delta T_{d,3}}{\Delta t} = \frac{\alpha_d}{(\Delta x)^2} (T_{d,2}^{n+1} - 2T_{d,3}^{n+1} + T_{d,4}^{n+1}), \quad (6)$$

and for the $T_{d,4}$ temperature point,

$$\frac{\Delta T_{d,4}}{\Delta t} = \frac{\alpha_d}{(\Delta x)^2} (T_{d,3}^{n+1} - 2T_{d,4}^{n+1} + T_{d,5}^{n+1}). \quad (7)$$

Around the first and fifth point, the discretized expressions of $\left(\frac{\partial^2 T}{\partial x^2} \right)$ result truncated and therefore were not used in this work.

Previous authors worked on the basis that the thermal properties of the die material are constant as the die temperatures do not reach the 200 °C [16]. However, from Eq. (6) and Eq. (7), the material properties

coefficient α_d dependence on the temperature can be obtained as every temperature $T_{d,2-5}$ involved on the equations are known from the thermocouples. In this study the hypothesis of a linear evolution of the properties with the temperature is assumed.

Once that the temperature on the surface of the die, $T_{d,1}$, is known, the heat flux through the die-workpiece interface, Q , is obtained. In this work and due to the lack of temperature points on the workpiece, the heat flux on the interface has been supposed equal to the heat flux between the surface of the die and the first thermocouple point,

$$Q \approx Q_{d,1-2}. \quad (8)$$

The heat flux between these two points can be calculated as

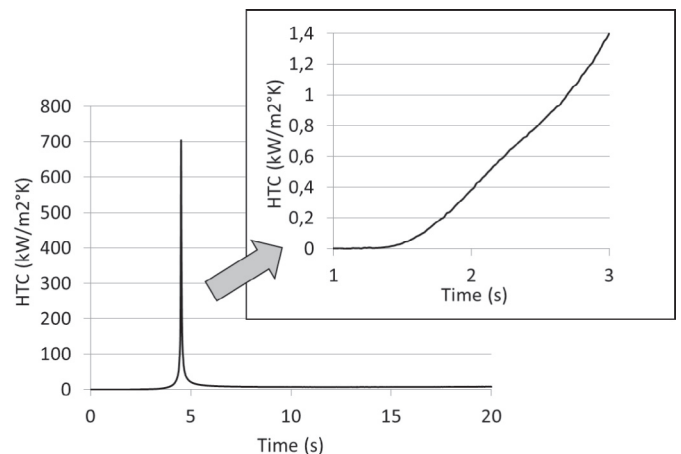


Fig. 4. Heat transfer coefficient evolution during the cooling process.

$$Q = k_d \frac{T_{d,1} - T_{d,2}}{\Delta x} \tag{9}$$

The thermal conductivity of the die material has been obtained by interpolating the supplier’s specifications with a second order polynomial

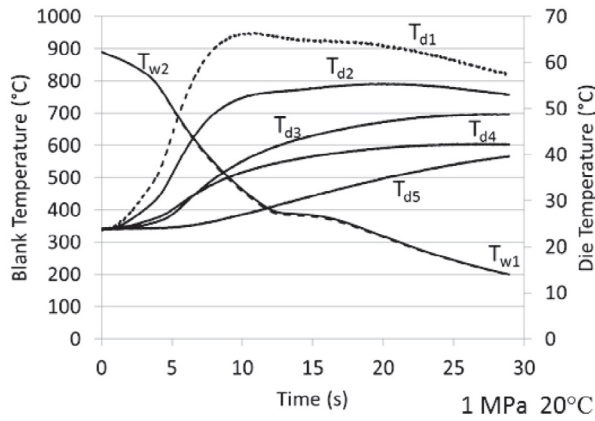
$$k_d = -9.528 \times 10^{-6} T^2 + 1.453 \times 10^{-2} T + 24.71, \tag{10}$$

where the temperature T has been taken on the surface of the die.

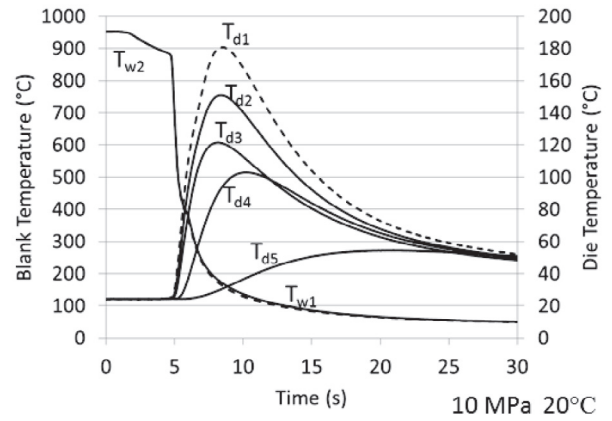
In order to obtain the temperature on the surface of the workpiece the hypothesis of constant flux from the workpiece to the die has been used on this work,

$$Q \approx Q_{w,1-2}, \tag{11}$$

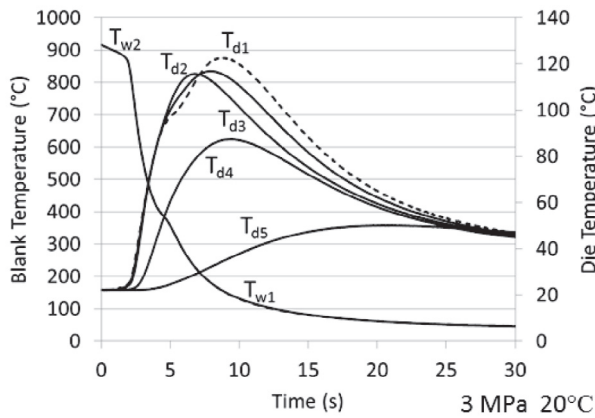
where $Q_{w,1-2}$ is the heat flux between the $T_{w,2}$ temperature point and the surface of workpiece, $T_{w,1}$. The temperature difference between the surface and the thermocouple point, $\Delta T_{w,1-2}$, can be therefore calculated as



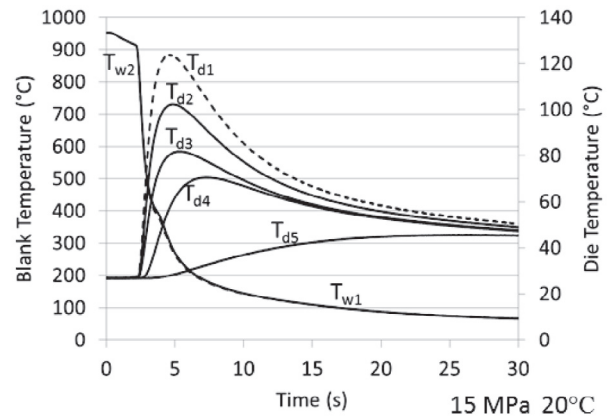
(a)



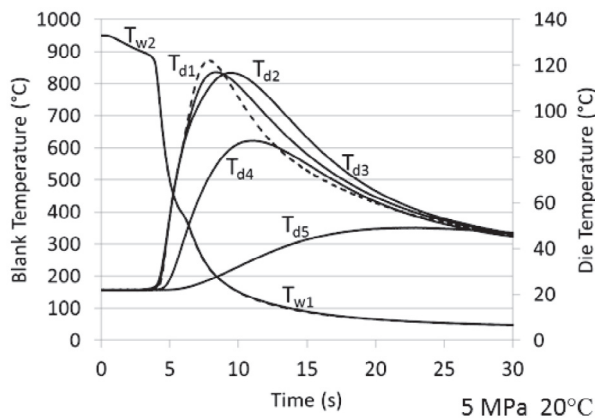
(d)



(b)



(e)



(c)

Fig. 5. Temperature evolution under different contact pressures with an ambient temperature condition die.

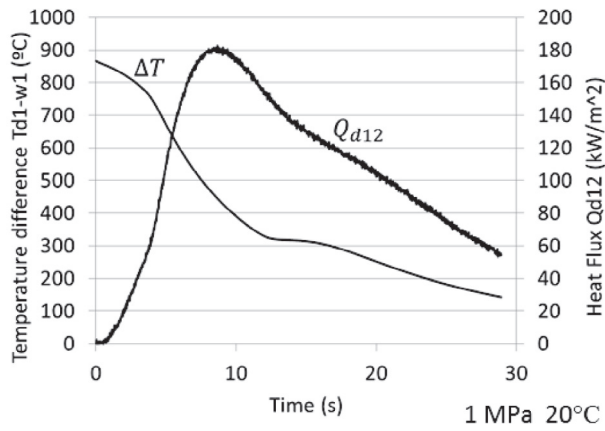
$$\Delta T_{w,1-2} = \frac{Q_{w,1-2}\Delta y}{k_w}, \tag{12}$$

where Δy represents the distance between the $T_{w,2}$ temperature point and the surface of the workpiece and k_w is the thermal conductivity of the workpiece. The thermal conductivity of the USIBOR 1500P was studied by previous authors and its properties are summarized on Table 2.

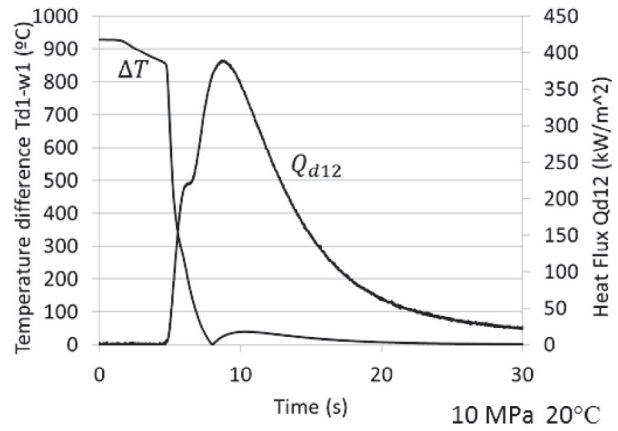
During the quenching step, the microstructure of the workpiece changes from austenite to martensite and therefore the thermal conductivity is dependent on that transformation as,

$$k_w = f_m k_{w,m} + (1 - f_m) k_{w,a}, \tag{13}$$

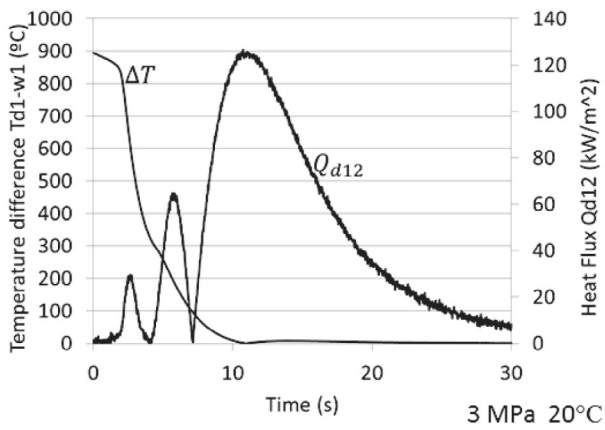
where $k_{w,m}$ and $k_{w,a}$ are the thermal conductivity of the martensite and austenite respectively (Table 2). On the other hand, the



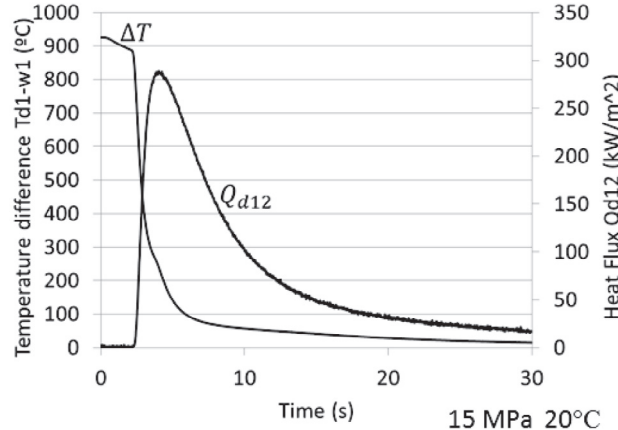
(a)



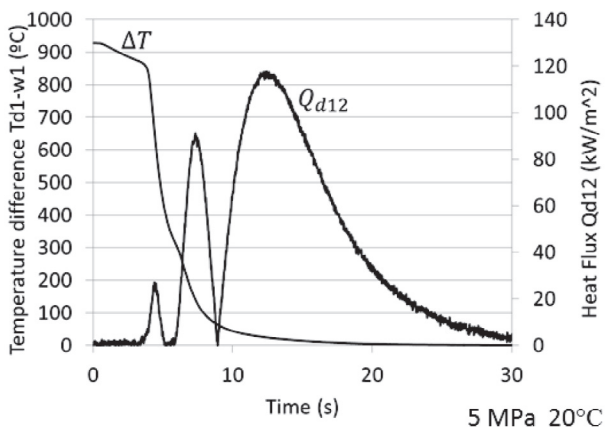
(d)



(b)



(e)



(c)

Fig. 6. Resultant flux and temperature difference on the interface under different contact pressures with an ambient temperature condition die.

martensite volume fraction, f_m , can be expressed dependent of the temperature,

$$f_m = 1 - \exp(-0.011(673 - T)), \quad (14)$$

where it is set to zero for workpiece temperatures above 673 °K.

4. Results

By using the above presented methodology the temperature on both surfaces and the heat flux during the cooling process has been calculated for all experiments.

4.1. Heat transfer coefficient experimental results

Fig. 3 shows the characteristic results of a HTC experimental test. The temperatures on the thermocouples and the calculated temperatures on the surfaces are shown in Fig. 3a. Being a thin sample, both the temperature on the middle of the thickness, $T_{w,2}$, and the calculated temperature on the surface, $T_{w,1}$, are really close. However, an important temperature difference can be appreciated between the surface of the die and the thermocouple readings in the die.

Fig. 3b shows the temperature difference (in absolute values) between the interface surfaces as well as the heat flux. The initial temperature difference is about 890–930 °C (915 °C to 950 °C on the blank with a die at 20 °C) and it takes around 4 seconds (in this particular case) to reach the convergence to the temperature of the die. The heat flux on the other hand starts with a low value and increases during the process reaching its maximum value around 4–5 s after the initial contact. This phenomenon is due to the kinetics of the heat transfer and it was previously observed by other authors as [7]. The same effect was shown in both the study of Abdulhay et al. [13] in their work of HTC characterization and on the flux difference and thermocouple response analysis conducted by Caron et al. [18].

As previously authors stated, a singularity can be observed in all results around the microstructural change zone. This singularity is more obvious on the flux representation (Fig. 3b) but it is present as well on the temperature results (Fig. 3a and 3b) and it is related with the latent heat during the transformation [13].

By computing the HTC using the expression shown in Eq. (1), the HTC results to the ratio between the heat flux and the temperature difference. The characteristic result of the HTC is shown in Fig. 4 (these HTC has been calculated using the data of Fig. 3b).

The fast decrease of the temperature difference and the slow increase of the flux during the cooling process leads to a variable HTC with an important pick value around the maximum flux point.

4.1.1. Effect of the applied pressure on the HTC evolution

The temperature evolution on the thermocouples and the calculated temperatures on the surfaces under different contact pressures are presented in Fig. 5.

The singularity due to the microstructure change is clearly shown in all blank temperature evolution results. In the same way, the influence of the contact pressure on the temperature exchange rate is shown as the lower the pressure is, the longer the cooling time results (on the analysed 1 MPa to 15 MPa pressure range).

Fig. 6 shows the temperature difference between the die and the blank and the resultant heat flux for the experiments shown in Fig. 5.

The increase of the temperature exchange rate is well shown in Fig. 6 where the time needed to reach the 200 °C of difference is reduced when the pressure increases. This time is critical in a press hardening operation being around 250 °C where the full martensitic transformation is finished.

The calculated HTC value for the different contact pressures dependent on the temperature difference is shown in Fig. 7. The HTC

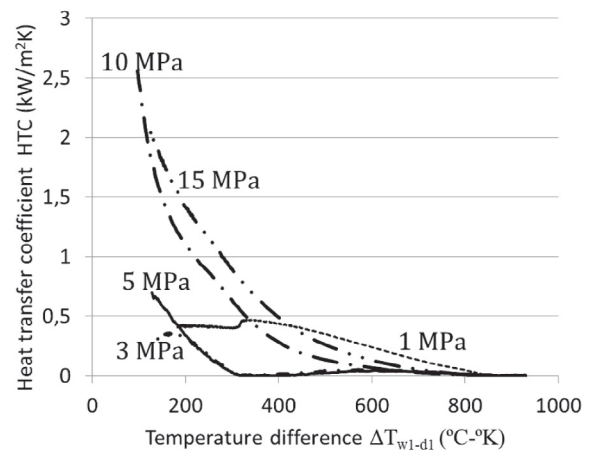


Fig. 7. Heat transfer coefficient evolution under different contact pressures represented against the interface temperature difference.

evolution has been truncated when 250 °C on the blank is reached (this is the point in which the microstructure has been fully modified).

Two main conclusions can be drawn from these results. On the one hand, there is the increase of the HTC with the applied pressure (on the 1 MPa to 15 MPa pressure range). This phenomenon has been previously related with microplasticity and the increase of the effective contact area in other heat transfer problems and materials out of the press hardening field [18]. As it is shown in Fig. 8, the applied pressure plastically deforms the asperities of the surfaces and in this way the effective contact area is increased.

On the other hand is the fact that the HTC is not constant and varies during the cooling process. This is a critical result as the state of the art of the HTC in press hardening is limited to constant HTC values [17] and this simplification could lead to different cooling ratios and therefore microstructures.

As previously presented for room temperature dies, Fig. 9 shows the temperature evolution during the HTC tests carried out under 450 °C die temperatures. These results will help to understand the heat kinetics happening in automotive tailor quenched component manufacturing [4].

Due to the high temperature of the die the temperature exchange rate is lower than that of room temperature dies. Therefore, longer times are needed to reach the die temperature on the blank. However, the same increase in that exchange rate is shown when increasing the applied pressure.

Fig. 10 on the other hand shows the temperature difference and heat flux for high die temperature testing.

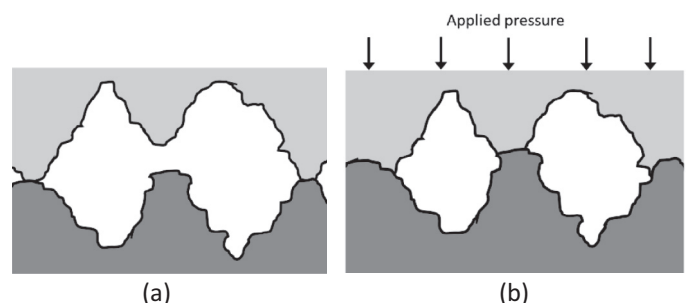


Fig. 8. Surface microplasticity influence on the increase of the effective contact area.

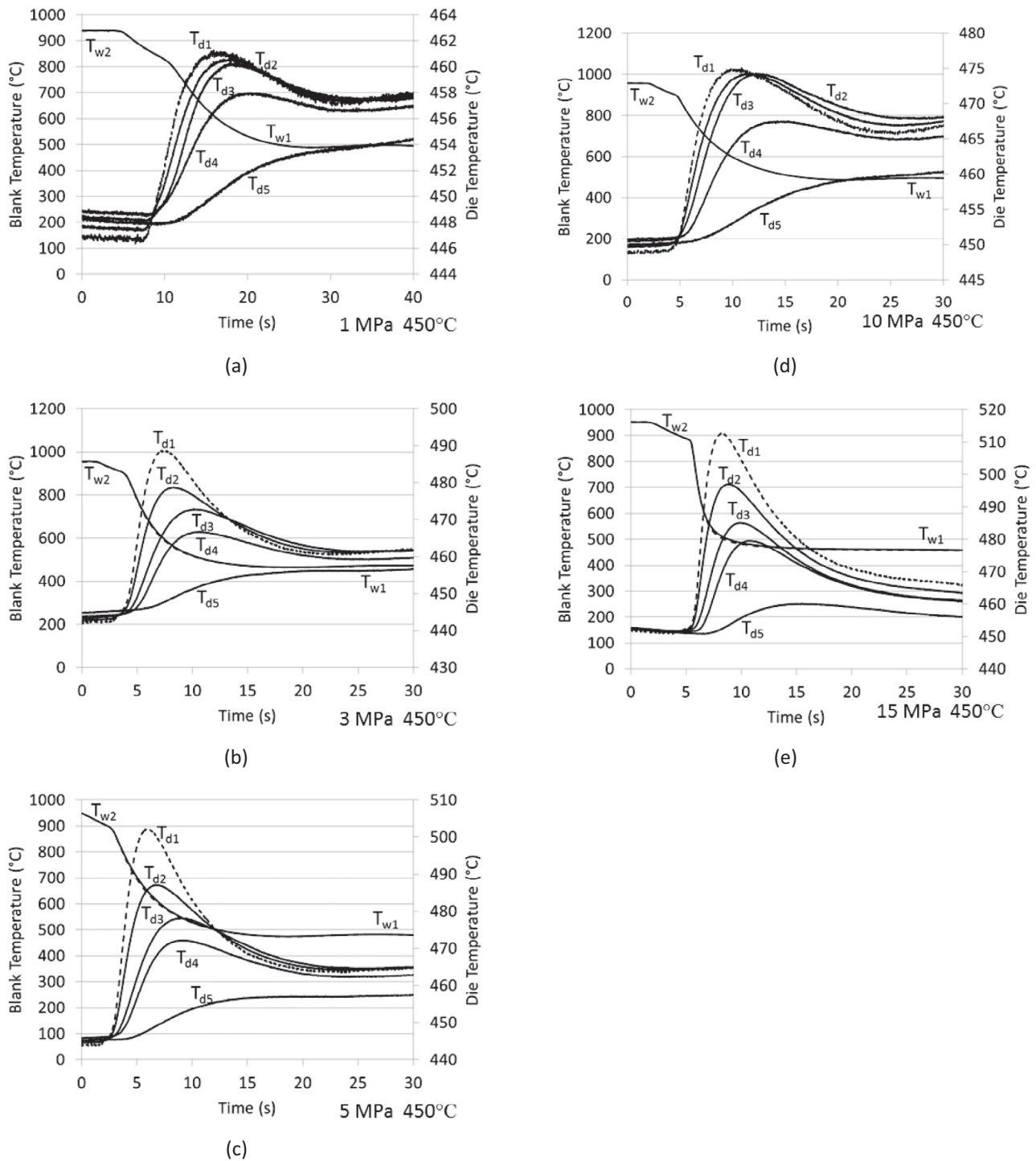


Fig. 9. Temperature evolution under different contact pressures with a high temperature die.

In these results the singularity of the microstructural change is not appreciated and this is due to the fact that the martensite transformation starts at 673 K (400 °C).

Fig. 11 shows the HTC value obtained in these tests where high die temperatures are used.

An asymptotic increase of the HTC is observed for 15 MPa of applied pressure but there is no clear tendency of the results observed for the other pressures as shown for room temperature data.

In order to analyse the effect of the die temperature on the cooling

process, experiments were carried out under intermediate 80 °C, 200 °C and 300 °C temperatures under 10 MPa of pressure. Figs. 12 and 13 show the temperature evolution during the test and the temperature difference and flux respectively.

As previously concluded the increase of the die temperatures decreases the temperature exchange rate and increases the cooling time.

The influence of the die temperature on the evolution of the HTC is presented in Fig. 14. Similar to the results of Fig. 11, the HTC evolutions for die temperatures above 200 °C do not show the

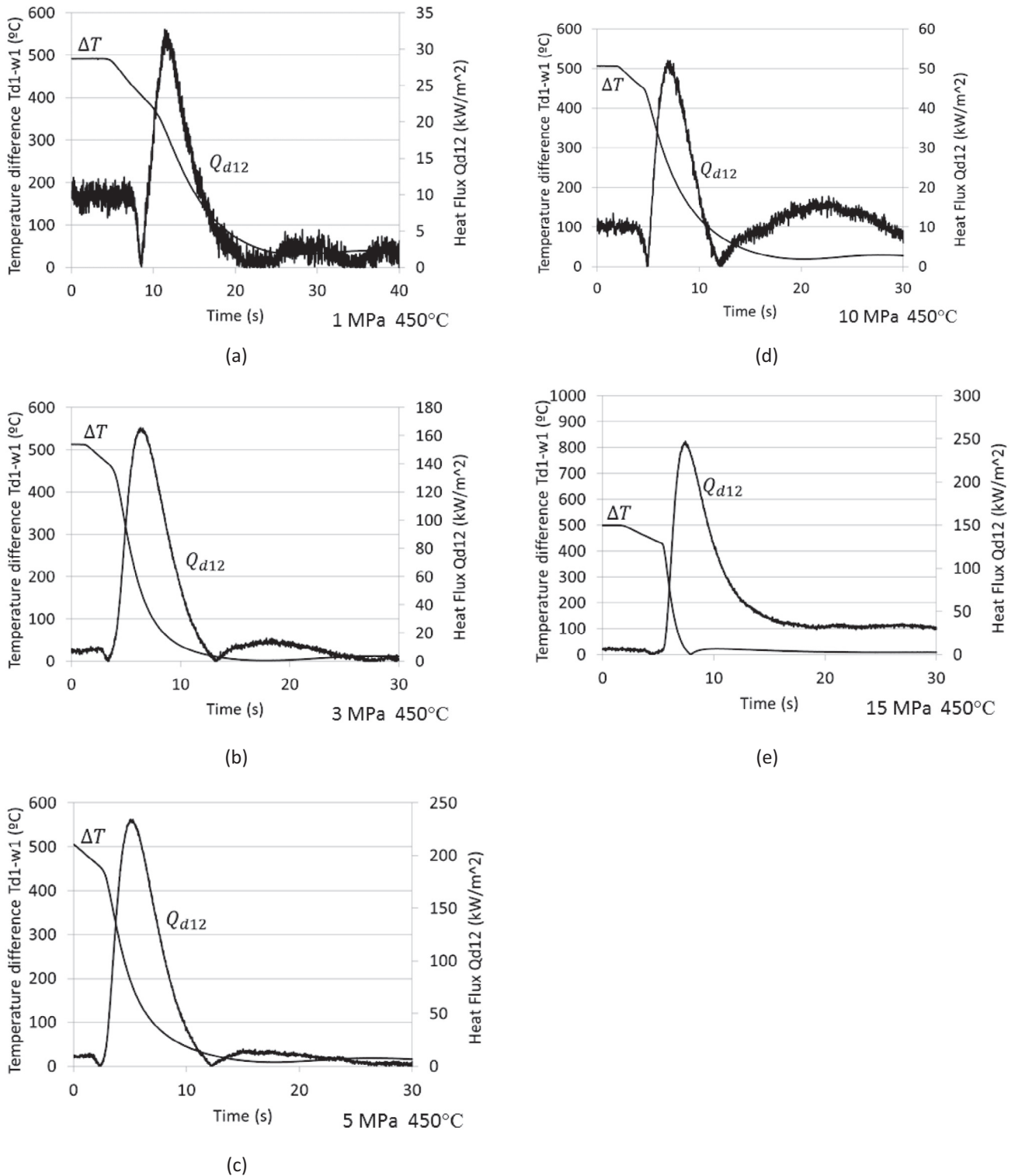


Fig. 10. Resultant flux and temperature difference on the interface under different contact pressures with a high temperature die.

characteristic asymptotic tendency on the analysed die temperatures from 24 °C to 450 °C.

However, when comparing the results obtained for die temperatures of 20 °C, 80 °C and 200 °C, all experimental show the same evolution of HTC (function of the temperature difference between the contact surfaces).

4.2. Modified heat transfer coefficient experimental results

Nowadays, the commercial software for press hardening numerical simulations usually assumes a constant temperature of the die. This is due to the fact that analytical (or discrete) rigid tools are used to improve the computational time.

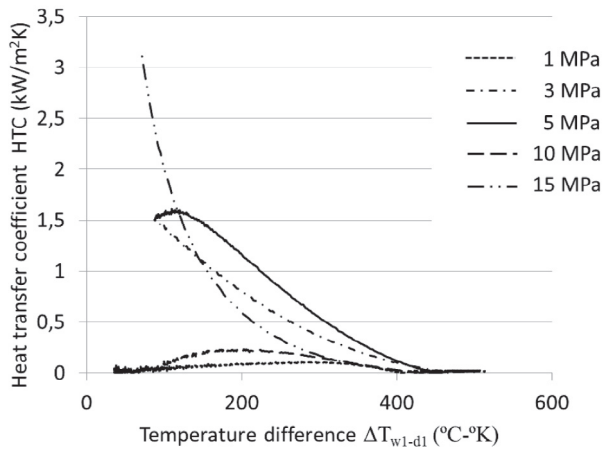


Fig. 11. Heat transfer coefficient evolution under different pressures with a high temperature die.

The previously presented results show an evolution of the die temperatures during the process while the HTC values were presented depending on the temperature difference between the die and the blank.

In order to provide valid HTC values for the industry, a modified heat transfer coefficient (HTC*) has been calculated to be used in commercial press hardening software. This HTC* was calculated to reproduce the experimental temperature decrease on the blank assuming a constant 80 °C of temperature on the die during the whole process.

$$HTC^* = \frac{Q}{T_{w1} - 80^{\circ}C} \tag{15}$$

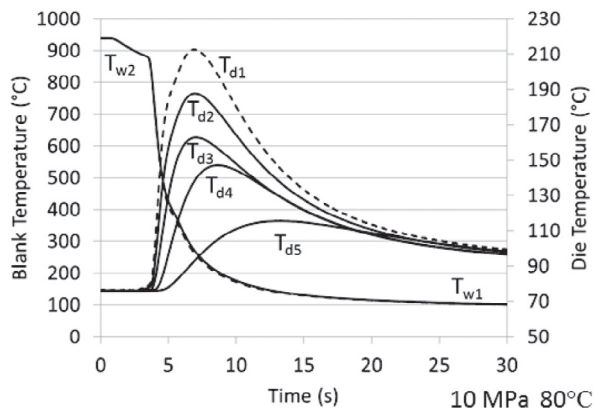
The closing pressures in an industrial press hardening operation are between 8 MPa and 15 MPa. That is why, in order to provide a useful tool to the industry, a model has been fit to the modified heat transfer coefficient (HTC*) experimental values of 5 MPa, 10 MPa and 15 MPa. Fig. 15 shows the HTC* values of 5 MPa, 10 MPa and 15 MPa where the temperature difference T_{w1-d1} represents the difference between the blank temperature and 80 °C. In the figure, the experimental data is shown in markers while the model prediction is represented by a continuous line following

$$HTC^* = A - B(1 - e^{-C(\Delta T^* - 200)}), \tag{16}$$

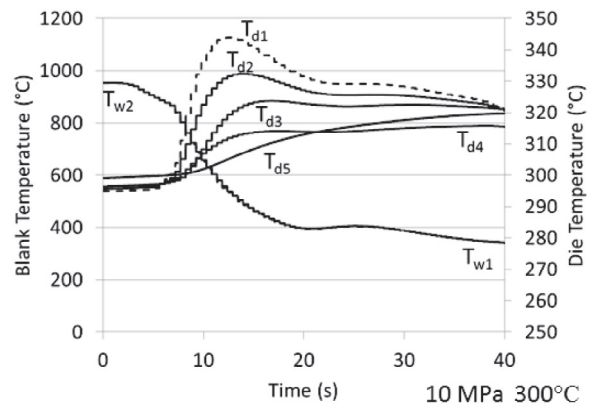
where,

$$C = (-0.2 p^2 + 3 p + 45) \cdot 10^{-4}, \tag{17}$$

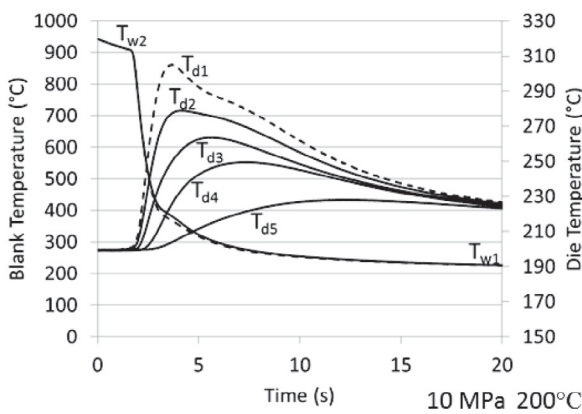
$$A = 0.0114 p^2 - 0.1392 p + 0.9108, \tag{18}$$



(a)

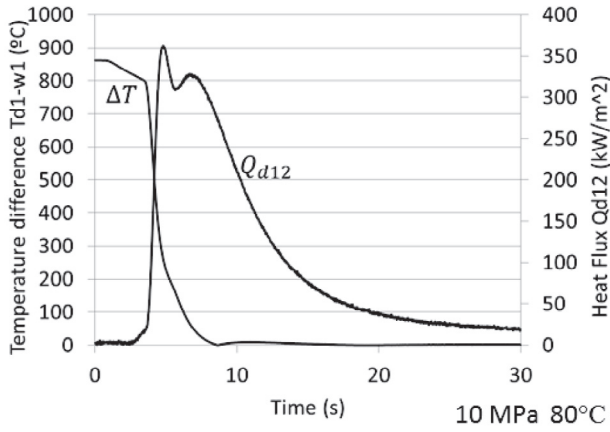


(c)

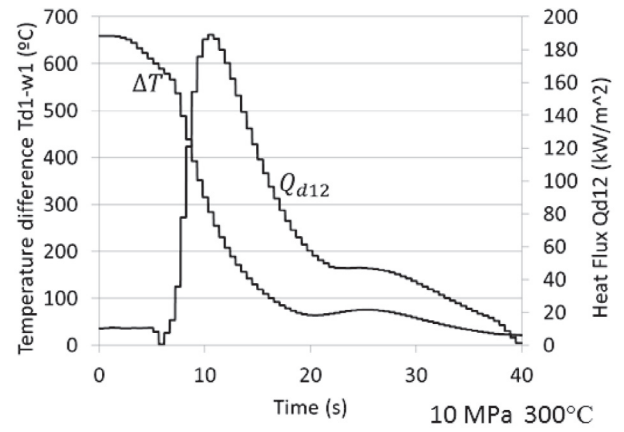


(b)

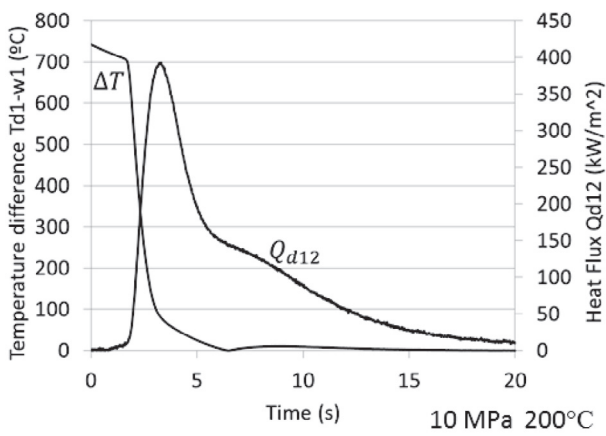
Fig. 12. Temperature evolution under different die temperatures.



(a)



(c)



(b)

Fig. 13. Resultant flux and temperature difference on the interface under different die temperatures.

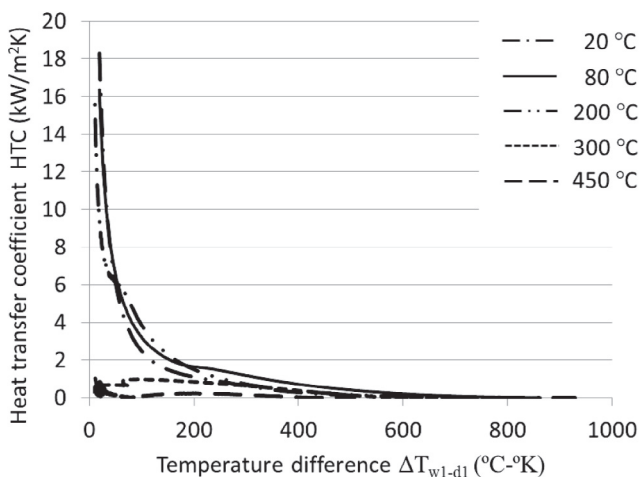


Fig. 14. Heat transfer coefficient evolution under different die temperatures.

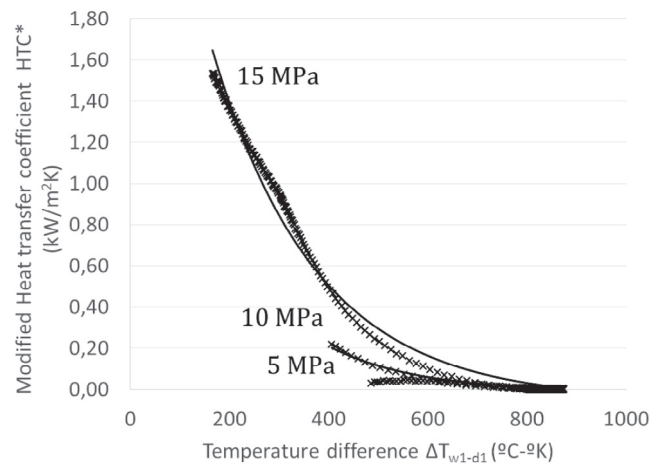


Fig. 15. Modified heat transfer coefficient evolution under constant 80 °C constant die temperature for 5 MPa, 10 MPa and 15 MPa. In markers the experimental data and in a continuous line the model prediction.

and where p represents the pressure. The value of the third constant is computed to assure the zero heat transfer coefficient at the beginning of the process,

$$B = \frac{A}{1 - e^{-C \cdot 670}} \quad (19)$$

The A coefficient represents the value of the HTC* at 200 degrees of temperature difference while the exponential tendency is controlled with the C coefficient.

5. Conclusions

The main conclusions that can be drawn from the presented research are:

- The HTC critically varies during the cooling process from the initial ~900 °C to the martensite transformation zone 400–250 °C
- Due to the heat kinetics (fast drop of the temperature difference and slow increase of the flux) a high pick can be observed on the HTC values
- Regardless the die temperature, the contact pressure increases the temperature exchange rate reducing the cooling time
- Above the 300 °C of die temperature the asymptotic nature of the HTC evolution is not observed
- The die temperature does not influence the HTC evolution (dependent on the temperature difference between the surfaces) on the analysed range of die temperatures from 24 °C to 450 °C
- Modified heat transfer coefficient HTC* were calculated for commercial press hardening software application

This work presents a valuable set of experimental data regarding the HTC characterization.

Acknowledgements

The authors thank the experimental work carried out by Jon Ander Lopez de Murillas Hurtado. Support from our industrial partner BATZ S.Coop. (IN-2012/00054), automotive tool maker, as well as the funding of the Basque Government (IN-2012/00054) to perform the Solintbo project is gratefully acknowledged.

References

- [1] Y. Abe, T. Ohmi, K. Mori, T. Masuda, Improvement of formability in Deep drawing of ultra-high strength Steel sheets by coating of die, *J. Mater. Process. Technol.* 214 (2014) 1838–1843.
- [2] J.Y. Lee, F. Barlat, M.G. Lee, Constitutive and friction modeling for accurate springback analysis of advanced high strength steel sheets, *Int. J. Plast.* 71 (2015) 113–135.
- [3] S. Sikora, F.J. Lenze, Hot-Forming-Process Important Parameters for the Production of High-Strength BIW Parts, *IDDRG, Porto, 2006*, pp. 295–301.
- [4] T.K. Eller, L. Greve, M.T. Andres, M. Medricky, A. Hatscher, V.T. Meinders, et al., Plasticity and fracture modeling of quench-hardenable boron steel with tailored properties, *J. Mater. Process. Technol.* 214 (2014) 1211–1227.
- [5] M. Merklein, J. Lachler, Investigation of the thermo-mechanical properties of hot stamping steels, *J. Mater. Process. Technol.* 177 (2006) 452–455.
- [6] H. Guler, R. Ozcan, Comparison of hot and cold stamping simulation of Usibor 1500 prototype model, *Indian J. Eng. Mater. Sci.* 21 (2014) 387–396.
- [7] H.S. Carslaw, Introduction to the Mathematical Theory of The conduction of Heat in Solids, Macmillan and Co, Limited St. Martin's Street, London, 1921.
- [8] J.G. Lenard, M.E. Davis, An experimental study of heat transfer in metal-forming processes, *CIRP Ann. Manuf. Technol.* 41 (1) (1992) 307–310.
- [9] Z. Malinowski, J.G. Lenard, M.E. Davies, A study of the heat-transfer coefficient as a function of temperature and pressure, *J. Mater. Process. Technol.* 41 (1994) 125–142.
- [10] C. Chang, A.N. Bramley, Determination of the heat transfer coefficient at the workpiece-die interface for the forging process, *Proc. Inst. Mech. Eng.* 216 (8) (2002) 1179–1186.
- [11] P. Salomonsson, M. Oldenburg, P. Akerstrom, G. Bergman, Experimental and numerical evaluation of the heat transfer coefficient in press hardening, *Steel Res. Int.* 80 (11) (2009) 841–845.
- [12] F. Tondini, P. Bosetti, S. Buschi, Heat transfer in hot stamping of high strength steel sheets, *Proc. Inst. Mech. Eng.* 225 (2011) 1813–1824.
- [13] B. Abdulhay, B. Bourouga, C. Dessain, G. Brun, J. Wilsius, Development of estimation procedure of contact heat transfer coefficient at the part-tool Interface in hot stamping process, *Heat Transfer Eng.* 32 (6) (2011) 497–505.
- [14] B. Abdulhay, B. Bourouga, C. Dessain, Experimental and theoretical study of thermal aspects of the hot stamping process, *Appl. Therm. Eng.* 31 (2011) 674–685.
- [15] Q. Bai, J. Lin, L. Zhan, T.A. Dean, D.S. Balint, Z. Zhang, An efficient closed-form method for determining interfacial heat transfer coefficient in metal forming, *Int. J. Mach. Tools Manuf.* 56 (2012) 102–110.
- [16] Q. Bai, J. Lin, L. Zhan, T.A. Dean, D.S. Balint, Z. Zhang, A new method for determining interfacial heat transfer coefficient and its application in hot/warm forming. Special Edition of Steel Research International, 14th Metal Forming International Conference on September 16–19, 2012, 2012, pp. 1035–1038.
- [17] M. Merklein, J. Lachler, Determination of material and process characteristics for hot stamping processes of quenchenable ultra high strength steels with respect to a FE-based process design, *SAE Int. J. Mater. Manuf.* 1 (2008) 411–426.
- [18] E. Caron, K.J. Daun, M.A. Wells, Experimental characterization of heat transfer coefficients during hot forming die quenching of boron steel, *Metall. Mater. Trans. B* 44 (2013) 332–343.
- [19] C. Wang, Y. Zhang, X. Tian, B. Zhu, J. Li, Thermal contact conductance estimation and experimental validation in hot stamping process, *Sci. China* 55 (7) (2012) 1852–1857.